Bioorganic & Medicinal Chemistry xxx (2015) xxx–xxx

Contents lists available at ScienceDirect

Bioorganic & Medicinal Chemistry

journal homepage: www.elsevier.com/locate/bmc

Synthesis and in vitro kinetic evaluation of *N*-thiazolylacetamido monoquaternary pyridinium oximes as reactivators of sarin, *O*-ethylsarin and VX inhibited human acetylcholinesterase (*h*AChE)

Aditya Kapil Valiveti [a], Uma M. Bhalerao [a], Jyotiranjan Acharya [a,*], Hitendra N. Karade [a], Badri Narayan Acharya [a], G. Raviraju [a], Anand K. Halve [b], Mahabir Parshad Kaushik [a]

[a] Process Technology Development Division, Defence Research & Development Establishment, Jhansi Road, Gwalior 474 002, India
[b] School of Studies in Chemistry, Jiwaji University, Gwalior, India

ARTICLE INFO

Article history:
Received 29 January 2015
Revised 13 May 2015
Accepted 15 May 2015
Available online xxxx

Keywords:
Acetylcholinesterase
Thiazolylacetamides
Nerve agents
Reactivation
Kinetics

ABSTRACT

Presently available medications for treatment of organiphosphorus poisoning are not sufficiently effective due to various pharmacological and toxicological reasons. In this regard, herein we report the synthesis of a series of *N*-thiazolylacetamide monoquaternary pyridinium oximes and its analogs (**1a**–**1b** to **6a**–**6b**) with diversely substituted thiazole ring and evaluation of their in vitro reactivation efficacies against nerve agent (sarin, *O*-ethylsarin and VX) inhibited human erythrocyte acetylcholinesterase (*h*AChE). Reactivation kinetics was performed to determine dissociation constant (K_D), reactivity rate constant (k_r) and the second order rate constant (k_{r2}) for all the compounds and compared their efficacies with commercial antidotes viz. 2-PAM and obidoxime. All the newly synthesized oximes were evaluated for their physicochemical parameters (p*K*a) and correlated with their respective reactivation efficacies to assess the capability of the oxime reactivator. Three of these novel compounds showed promising reactivation efficacies toward OP inhibited *h*AChE. Molecular docking studies were performed in order to correlate the reactivation efficacies with their interactions in the active site of the AChE.

1. Introduction

Organophosphorus compounds (OPs) have highly been industrialized owing to their wider applicability in the field of veterinary and human medicine, in the agriculture as pesticides and also have been misused for military purpose. The major revolution in the research of OPs began at the dawn of World War II that led to the accidental discoveries of various deadliest chemicals called nerve agents viz. sarin, soman, Tabun and VX[1] (Fig. 1). Owing to their acute toxicity toward mammalian systems these nerve agents have been used as chemical weapons of mass destruction in wars[2] as well as in the terrorist activities worldwide.[3] In addition, self-poisoning with OP pesticides is another important and current issue of global concern. Annually 300,000 deaths (either accidentally or intentionally) have been recorded due to the acute OP pesticide intoxications.[4] All these consequences strictly demand an effective medical treatment regimen against the acute OP-poisoning.

From the mechanism point of view the toxic OP compounds irreversibly bind to the serine hydroxyl group at the active site of enzyme AChE (AChE; E.C. 3.1.1.7). This results in elevated levels of ACh (acetylcholine; a neurotransmitter) at the pre- and post-synaptic junctions of the nerve ends. The unwanted accretion of ACh levels in peripheral and central nervous system leads to a variety of cholinergic manifestation that includes depression of respiratory center followed by peripheral neuromuscular blockade causing respiratory paralysis and death.[5] The behavior of phosphylated (represents, phosphonylation and phosphorylation) AChE is highly dependent on the structural variations and toxicity of the nerve agent used.[6] After inhibition, the OP–AChE adduct undergoes several biochemical pathways[7] viz., hydrolysis (with an effective nucleophilic attack at the P–O bond), spontaneous reactivation and aging process (in case of soman poisoning).[8] However, the recovery of original AChE activity to its normal functioning is highly essential to avoid the cholinergic break down and death.[9]

In general, the immediate therapeutic intervention for acute OP nerve agent poisoning involves administration of an anti-muscarinic agent (atropine),[10] anti-convulsant (Diazepam)[11] and enzyme reactivator oximes (Fig. 2; 2-PAM, Obidoxime and HI-6).[12,13]

* Corresponding author. Tel.: +91 751 2390205, +91 751 2340245; fax: +91 751 2341148.
E-mail addresses: jracharya01@gmail.com, j.acharya@drde.drdo.in (J. Acharya).

http://dx.doi.org/10.1016/j.bmc.2015.05.027
0968-0896/

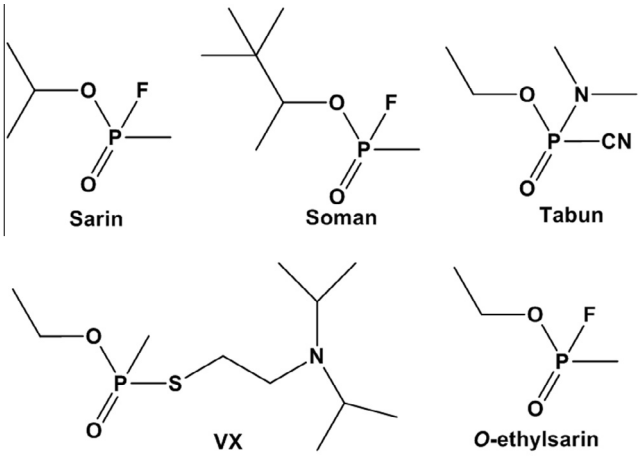

Figure 1. Structure of the organophosphorus nerve agents.

There are several factors which limit the scope of oxime therapy in the context of acute OP poisoning. Being quaternary ammonium salts, majority of these oximes are unable to cross the blood brain barrier.[14,15] Further, oxime treatments are ineffective toward the aged enzyme. Moreover, the intrinsic toxicities of these oximes exert deleterious side effects.[16,17] All these drawbacks strictly underscore the need of a versatile antidotal treatment in the event of acute OP nerve agent and pesticide poisoning.[18] Over past few decades, numerous structurally divergent oxime reactivators were synthesized and evaluated for their efficacies against acute OP poisoning.[19–27] As newly synthesized compounds cannot be evaluated on humans for ethical reasons hence studies on animals and human enzymes are the mainstay for understanding the pharmacological and toxicological interactions between the antidotes and the OP–enzyme complexes.[28–30] In the development of versatile and effective medical countermeasures against acute OP poisoning, extensive variations in the structural features of oxime reactivators are needed for further refinement to shape-up a broad spectrum antidote.[31,32]

2. Synthesis and chemistry of *N*-thiazolylacetamido pyridinium oximes

In continuation to our work on the development of antidotes against OP poisoning,[19,21] herein we report the synthesis and in vitro evaluation of a series of mono-pyridinium oximes having substituted thiazolylacetamides as side chain linkers. Thiazoles are aromatic and have most therapeutic access as drug candidates for various diseases.[31–36] These heterocyclic entities are capable of binding with specific enzyme targets and act as reversible inhibitors in the treatment of various neurological disorders.[37–39] In the present study, we have synthesized various thiazolylacetamides sandwiched between substituted phenyl group and the quaternary pyridinium moieties. These aromatic moieties in the reactivator were ensembled in order to facilitate various non-covalent interactions with the aromatic residues lined up along the rim of the gorge in the peripheral anionic site of AChE. Additionally the quaternary nitrogen in the pyridinium ring enables the cation-π interactions with the indole and imidazole based amino acid (Trp & His) residues present at the base of the AChE gorge.[40,41] The hydrogen bond donor and acceptor capability of the acetamido linkages between the thiazole and pyridinium rings may facilitate significant electrostatic interactions (hydrogen bonding, salt bridge and hydrophobicity) inside the narrow confines of the gorge which may aid in achieving proper orientations of the reactivator toward the phosphylated complex of AChE. Further, in vitro reactivation efficacies of the newly prepared oximes were tested against human erythrocyte AChE (*h*AChE) inhibited by three structurally different OPs viz. sarin, *O*-ethylsarin and VX.

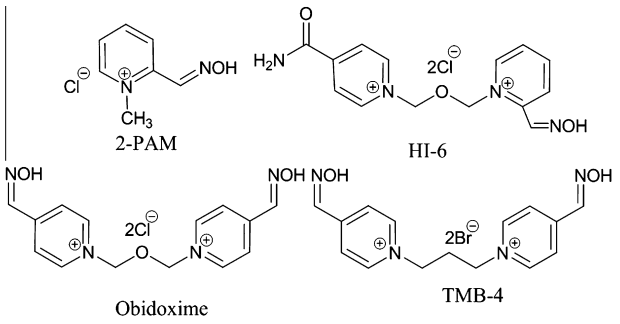

Figure 2. Structure of the pyridinium oxime reactivators.

3. Results

3.1. Reactivation of sarin inhibited *h*AChE

It was observed that the compounds containing oxime group at 4-position (**1a**–**6a**) of the pyridinium ring have shown better reactivation efficacy as compared to the compounds containing oxime group at 3-position (**1b**–**6b**) in case of sarin inhibition (Table 1). Variations in the K_D values of the oximes have been noticed and corroborated by their respective k_{r2} values (Table 1). Among all the 4-pyridinium compounds, oximes **6a**, **5a** and **3a** have shown considerable reactivation efficacies than other oximes as evident by their lower K_D (42.0 μM, 46.9 μM, 67.5 μM) and higher second order rate constant values k_{r2} (1.70 mM^{-1} min^{-1}, 1.60 mM^{-1} min^{-1}, 1.04 mM^{-1} min^{-1}). However, in case of 3-pyridinium oximes (**1b**–**6b**), higher K_D values have been observed which revealed their poor affinity and lower reactivity toward the OP–AChE adduct and hence resulted in lower k_{r2} values ranging from 0.14 to 0.68 mM^{-1} min^{-1}. Compound **3b** was the least efficacious and was unable to show any reactivation efficacy among all the oximes studied. Further, none of the synthesized oximes have been found to be effective than the standard oximes 2-PAM (k_{r2}; 2.95 mM^{-1} min^{-1}) and obidoxime (k_{r2}; 6.38 mM^{-1} min^{-1}). The overall reactivation efficacy order for all the oximes against sarin inhibited AChE was **obidoxime > 2-PAM > 6a > 5a > 3a > 1a > 2a > 5b > 1b > 4a > 6b > 2b > 4b > 3b**.

3.2. Reactivation of *O*-ethylsarin inhibited *h*AChE

In case of *O*-ethylsarin inhibited *h*AChE, except **4a**, majority of the oximes (having oxime at 4-position, **1a**–**6a**) have shown an appreciable reactivity toward the OP–AChE complex. It was observed that the oximes **6a**, **1a** and **5a** have higher reactivation efficacy as evidenced by their lower K_D (**6a**; 14.7 μM, **1a**; 29.9 μM and **5a**; 34.9 μM) and higher k_{r2} (**6a**; 4.31 mM^{-1} min^{-1}, **1a**; 2.66 mM^{-1} $min^{-1}$and **5a**; 2.05 mM^{-1} min^{-1}) values. In terms of both affinity and ability of the reactivator, oxime **6a** revealed better reactivation efficacy as compared to the standard oximes 2-PAM (k_{r2}; 2.19 mM^{-1} min^{-1}) and obidoxime (k_{r2}; 3.9 mM^{-1} min^{-1}). Further, oximes **3a** (50.6 μM) and **2a** (37.8 μM) have shown slightly lower affinities toward the phosphylated AChE in comparison to the oximes **6a**, **1a** and **5a**. However, these oximes have recorded lower reactivation efficacies as indicated by their lower k_{r2} values **3a**: 1.77 mM^{-1} min^{-1} and **2a**: 1.25 mM^{-1} min^{-1}, respectively (Table 1). Among the 4-positioned oximes, oxime **4a** was found to be least effective reactivator with higher K_D (90.6 μM; i.e., lower affinity) and lower k_{r2} (0.66 mM^{-1} min^{-1}) values.

Table 1
Reactivation constants for oxime-induced reactivation of OP-inhibited *h*AChE

Oxime	K_D μM (±SE)			k_r min^{-1} (±SE)			k_{r2} (mM^{-1} min^{-1})		
	Sarin	*O*-Ethylsarin	VX	Sarin	*O*-Ethylsarin	VX	Sarin	*O*-Ethylsarin	VX
1a	63.0 (11.5)	29.9 (7.3)	15.4 (2.2)	0.059 (0.003)	0.080 (0.004)	0.060 (0.002)	0.95	2.66	3.92
1b	115.0 (40.6)	87.6 (18.9)	98.3 (20.9)	0.076 (0.007)	0.079 (0.004)	0.095 (0.005)	0.66	0.89	0.96
2a	86.9 (10.4)	37.8 (9.7)	21.4 (5.1)	0.082 (0.002)	0.047 (0.003)	0.057 (0.003)	0.95	1.25	2.70
2b	682.7 (27.7)	762.6 (129.9)	350.6 (111.7)	0.129 (0.003)	0.129 (0.011)	0.094 (0.011)	0.19	0.17	0.27
3a	67.5 (25.2)	50.6 (14.1)	57.2 (15.5)	0.070 (0.006)	0.089 (0.005)	0.067 (0.004)	1.04	1.77	1.17
3b	nd	nd	145.6 (54.8)	nd	nd	0.056 (0.005)	nd	nd	0.38
4a	83.7 (25.4)	90.6 (25.6)	73.6 (17.8)	0.053 (0.004)	0.059 (0.004)	0.055 (0.003)	0.63	0.66	0.75
4b	641.0 (429)	nd	113.8 (14.9)	0.092 (0.029)	nd	0.097 (0.003)	0.14	nd	0.85
5a	46.9 (1.3)	34.9 (2.9)	12.9 (2.9)	0.075 (0.0005)	0.072 (0.001)	0.067 (0.002)	1.60	2.05	5.19
5b	109.2 (22.7)	104.5 (22.3)	97.7 (25.2)	0.074 (0.004)	0.079 (0.004)	0.086 (0.006)	0.68	0.76	0.88
6a	42.0 (4.4)	14.67 (3.0)	17.0 (4.4)	0.072 (0.002)	0.063 (0.002)	0.072(0.003)	1.70	4.31	4.23
6b	75.5 (24.8)	nd	58.4 (12.6)	0.046 (0.004)	nd	0.054 (0.003)	0.60	nd	0.92
2-PAM	28.8 (7.6)	34.7 (7.1)	17.77 (69.7)	0.085 (0.005)	0.076 (0.003)	0.070 (0.003)	2.95	2.19	3.92
Obid.	19.5 (4.6)	20.2 (5.8)	14.4 (3.0)	0.125 (0.005)	0.079 (0.004)	0.129 (0.005)	6.38	3.9	9.03

nd: not determined.

Decrements in the reactivation efficacies were observed in case of 3-pyridinium oxime derivatives **1b–6b**. Majority of the oximes (**3b**, **4b** and **6b**) failed to reactivate the OP inhibited *h*AChE in the 60 min course of the reactivation due to their poor affinity toward the tetrahedral complex of OP and *h*AChE. Again, oximes **1b**, **5b** and **2b** showed poor reactivation efficacies as represented by their lower second order rate constant k_{r2} values (0.89 mM^{-1} min^{-1}, 0.76 mM^{-1} min^{-1}, 0.17 mM^{-1} min^{-1}). Among these, **2b** was the least effective reactivator with the highest K_D (762.6 μM) value.

3.3. Reactivation of VX inhibited *h*AChE

The ability of all the tested oximes to reactivate the VX inhibited *h*AChE has been presented in Table 1. It was worth noticing that in case of VX inhibited *h*AChE, reactivation efficacy was significantly higher compared to other OP agents (sarin and *O*-ethylsarin) used in this study. Among the 4-positioned oximes (**1a–6a**), oximes **5a** and **6a** have shown higher reactivation efficacies as revealed by their lower K_D values: 12.89 μM and 17.0 μM and higher k_{r2} values: 5.19 mM^{-1} min^{-1} and 4.23 mM^{-1} min^{-1}, respectively than the standard oxime 2-PAM. In addition, oximes **1a** (k_{r2}; 3.92 mM^{-1} min^{-1}) and **2a** (k_{r2}; 2.70 mM^{-1} min^{-1}) have also shown comparable reactivation efficacies to that of 2-PAM. Oxime **4a** with highest dissociation constant K_D (73.6 μM) and lowest k_{r2} values (0.75 mM^{-1} min^{-1}) was found to be least effective in case of VX inhibited *h*AChE. Further, 3-pyridinium oximes (**1b–6b**) demonstrated lower reactivation efficacies as evident from their higher K_D and lower k_{r2} values. Among these, oximes **1b**, **6b**, **5b** and **4b** have shown much less k_{r2} (0.96 mM^{-1} min^{-1}; 0.92 mM^{-1} min^{-1}; 0.88 mM^{-1} min^{-1}; 0.85 mM^{-1} min^{-1}, respectively) values revealing their insignificant efficacies toward VX inhibited *h*AChE. Oxime **2b** was found to be the least effective reactivator among all the synthesized oximes with highest K_D (350.6 μM) and least k_{r2} (0.27 mM^{-1} min^{-1}) values.

The relative time and concentration dependent reactivation profile of oxime **5a** and the plot of k_{obs} against oxime concentration for all the three OP inhibitors were depicted in Figure 3.

4. Discussion

Determination of kinetic parameters and in vitro experiments has extensively been used in the assessment of the reactivation efficacies of newly synthesized oximes. These kinetic parameters have also been used to establish the correlation between the structure of the inhibitor and reactivation ability of new oxime reactivators.[6,28,42–44] Therefore determination of the kinetic parameters were of paramount importance to understand the mechanism of oxime and inhibitor interactions within the AChE active site.[42] In this investigation, three structurally divergent OP inhibitors have been used to study variations in the reactivation efficacy of the newly synthesized oximes. The reactivation kinetics data were generated by performing experiments under identical experimental protocols as reported in the literature 6.

The findings of the present study demonstrated that the position of the oxime group in the pyridinium ring was a significant factor in assessing the affinity, ability and the specific reactivity of the oxime reactivator. Marked differences were noticed with respect to their kinetic parameters among the tested oximes. The improved reactivation efficacies in terms of affinity toward the phosphylated AChE complex was observed in case of VX and *O*-ethylsarin inhibited *h*AChE compared to that of sarin inhibition.

Majority of the compounds containing oxime at 4-position (**1a–6a**) have shown greater reactivation efficacy as compared to the compounds containing oxime at 3-position (**1b–6b**) of the pyridinium ring. This finding inferred that the position of the oxime moiety in the pyridinium ring was a critical factor in deciding the ability of the oxime as reactivator. The overall reactivating potencies of all the tested oximes against the three OP nerve agents followed the order VX > *O*-ethylsarin > sarin. The percentage reactivation efficacy for all the tested oximes (**1a–6a** and **1b–6b**) in comparison to 2-PAM and obidoxime at 60 minute against the nerve agents (sarin, *O*-ethylsarin and VX) has been illustrated in Figure 4.

It was found that the standard obidoxime has shown better reactivation efficacy toward all the three nerve agents inhibited *h*AChE. Being bis-pyridinium in nature, the presence of a second quaternary center in the obidoxime molecule might be responsible for their higher binding affinity toward OP–AChE complex in the active site of the enzyme gorge. This has resulted in higher rate constant and reactivity of obidoxime toward OP inhibited AChE. In contrast, in the present investigation all the studied oximes were of mono-quaternary in nature. These oximes were chosen with an aim of enhancing the hydrophobicity of the reactivator and also to observe the presence of non-covalent interactions (if any) viz. cation–π, π–π and hydrogen boding interactions with the aromatic amino acid residues present inside the gorge of AChE.

The variations observed in the reactivation abilities of the oximes used in this study might be due to the discrepancy in the occupied molecular volumes of the tested OP inhibitors in the active site of AChE. The difference in the molecular volumes could be due to the presence of *O*-alkyl substituent in the OP inhibitors. In case of VX and *O*-ethylsarin, after the departure of their respective

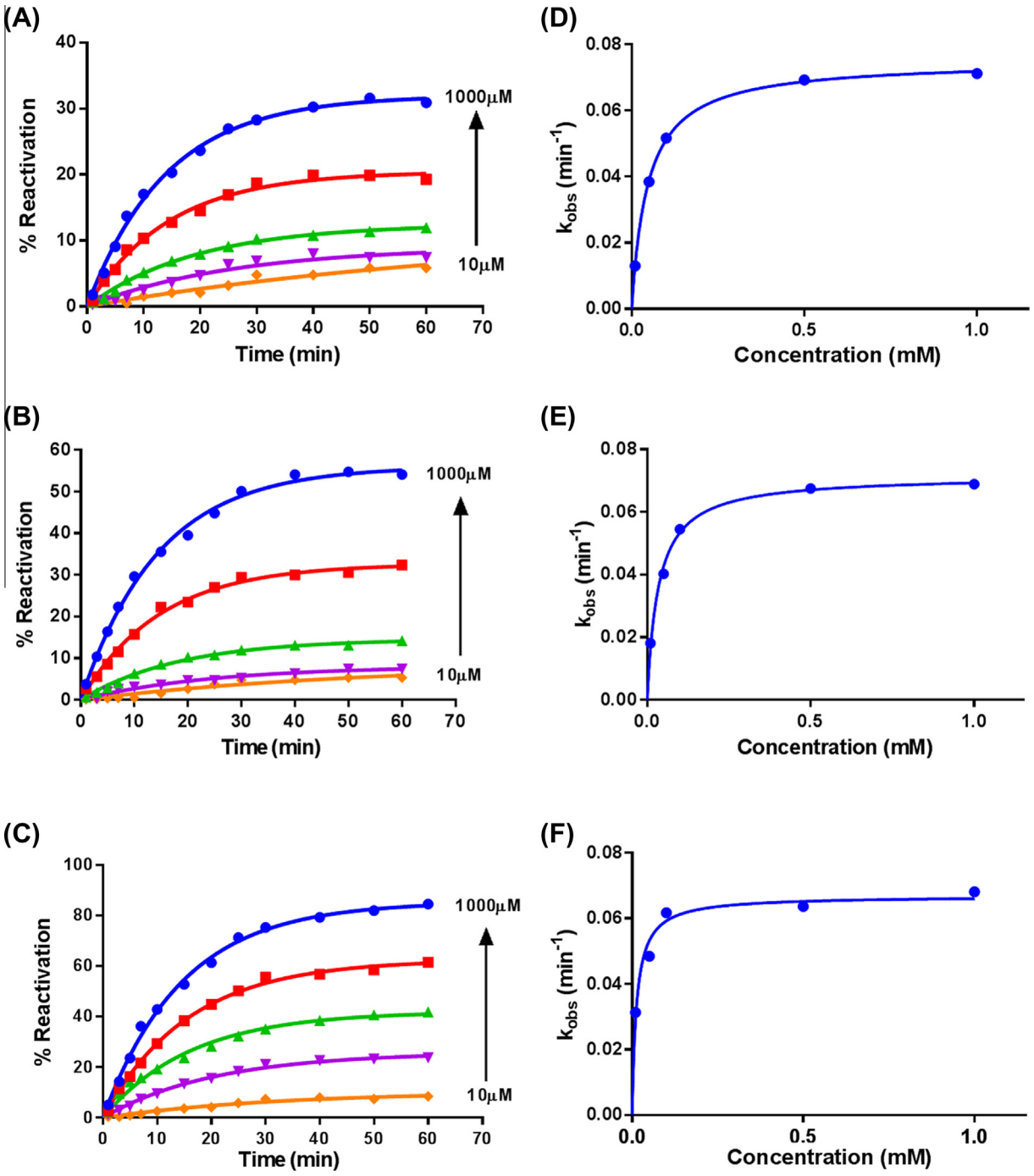

Figure 3. Relative time and concentration dependent reactivation profile of oxime **5a** against (A) sarin, (B) *O*-ethylsarin and (C) VX inhibited human AChE (A–C). Corresponding plot of k_{obs} against oxime concentration [**5a**] (D–F). Data are means of ±SE, $n = 2$.

leaving groups the formed OP–AChE adducts were structurally same as compared to the sarin-AChE conjugate (Scheme 1). Hence, the active site of the AChE gorge was mainly occupied by the bulky isopropyl group of the sarin followed by the *O*-ethyl group of the VX and *O*-ethylsarin.[44] Therefore the active site of AChE inhibited by VX and *O*-ethylsarin was least occupied and hence there might be greater access of the incoming nucleophile (oxime) toward the P-atom. This could be the plausible explanation that majority of the oximes have shown greater affinity (K_D) and ability (k_{r2}) to reactivate the VX followed by *O*-ethylsarin inhibited *h*AChE (oxime **5a**, **6a** and **1a**; Table 1). However, no similar trends have been observed in the reactivation profiles of the tested oximes in case of VX and *O*-ethylsarin inhibition. This could be due to unknown pharmacological or toxicological implications which remain to be explored.

In the past, several reactivators linked with heterocyclic side chains to the pyridinium ring were reported in order to augment various interactions of the oxime moiety with π-stacking clouds of the amino acid residues present inside the 20 Å deep gorge of AChE. Docking studies and calculation of binding energies performed on these type oximes revealed the importance of the various non-covalent interactions viz. hydrogen bonding, cation–π and π–π interactions that influenced the reactivation efficacy of the reactivators.[20,23–25] In this study, heteroaromatic thiazoles

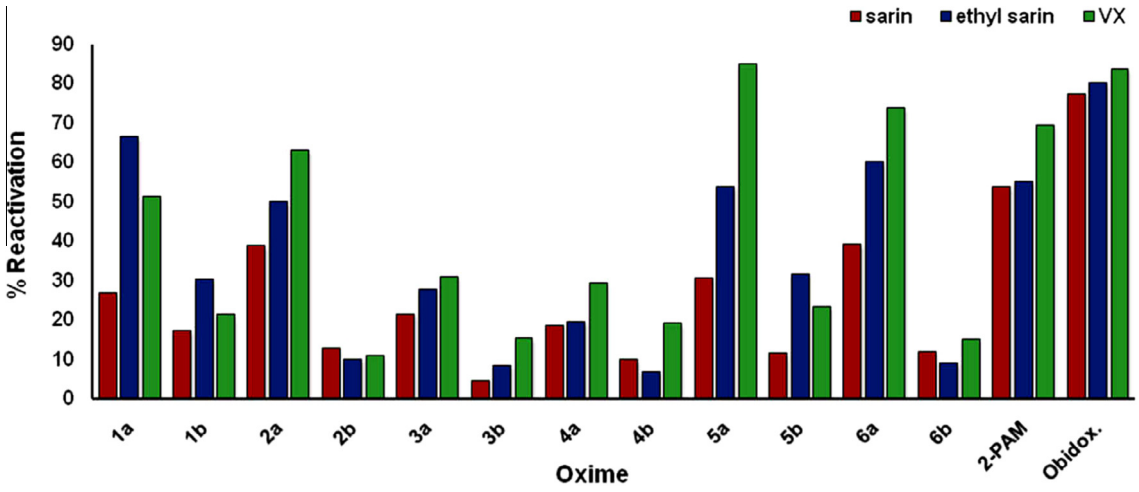

Figure 4. Percentage reactivation efficacies (%) of the oximes (**1a**–**6a** and **1b**–**6b**) in comparison to 2-PAM and obidoxime against OP-inhibited *h*AChE. Oxime concentration: 1 mM, pH: 7.4 and temperature: 37 °C.

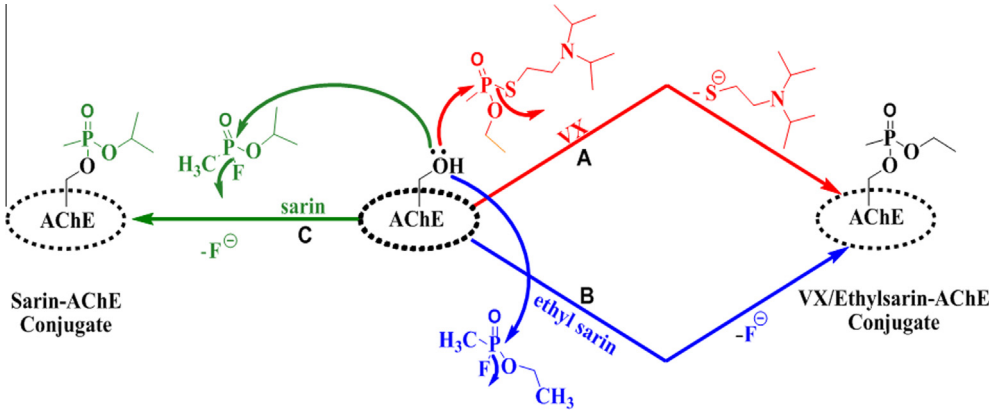

Scheme 1. Comparative inhibition process of AChE by (a) VX (b) *O*-ethylsarin and (c) sarin.

possessing extended conjugation with aromatic rings were incorporated in to the pyridinium oximes in order to observe the effect of aromatic clouds on the orientation and reactivation of the reactivator. Oximes **5a** and **6a** showed highest reactivation efficacy in case of VX and *O*-ethylsarin inhibited AChE as indicated by their lowest K_D value and highest second order rate constant k_{r2} than any other tested oximes (Table 1). Therefore, oximes with ester substituted thiazole linker might have imparted a better orientation toward the phosphylated AChE complex in the active site of the gorge. This could be the plausible reason that among all the synthesized oximes, the ester substituted thiazole linkers (**5a** and **6a**) have shown superior reactivation efficacies and improved affinities in case of *O*-ethylsarin and VX inhibited AChE. Therefore oximes **5a** and **6a** were further subjected for docking studies with nerve agent modified human AChE in order to understand their superior reactivation efficacy. The average binding energies for **5a** and **6a** were presented in Table 2. Both the oximes have interacted in a similar manner with the active site of the inhibited enzyme through hydrogen bonding (H-bonding). In Figure 5, it can be seen that, the flexible amide linker attached to the thiazole moiety facilitates the orientations of the ligand in the active site of the AChE mainly through H-bonding (green dotted lines). The H-bonding interactions are primarily observed between various amino acid residues of AChE and the amide linker as well as the carbonyl oxygen of the ester tail linked to the thiazole moiety.

Table 2
Binding energy values of oxime **5a** and **6a** bound to the sarin, VX/*O*-ethylsarin modified *h*AChE

Oxime	Binding energy (Kcal/mol)	
	Sarin inhibited AChE	VX/Ethyl sarin inhibited AChE
5a	−9.76	−11.74
6a	−10.69	−11.31

In case of sarin modified AChE, it was noticed that the oxime **5a** has two H-bonding interactions with TYR 337 residue. Another H-bonding was observed between the nitrogen atom of the oxime group of **5a** and PHE 295 (Fig. 5A). **6a** has one H-bonding between TYR 337 and the nitrogen atom of the thiazole ring. In addition another interaction was observed between HIS 447 and the nitrogen atom of oxime functionality (Fig. 5B). Even having one H-bond less, **6a** has shown better binding energy than **5a**. The greater size of **5a** responsible for higher conformation energy resulted due to steric hindrance with nearby amino acid residues of AChE than **6a**. This might be the reason for the greater reactivation efficacy of **6a** in case of sarin inhibited *h*AChE. This was further manifested by better rate constant of **6a** against sarin inhibited *h*AChE. In case of VX/*O*-ethylsarin modified AChE, **5a** has H-bondings between the carbonyl group of the amide linkage and the NH dipole of the amide group with amino acid residues TYR 337 and TYR 124,

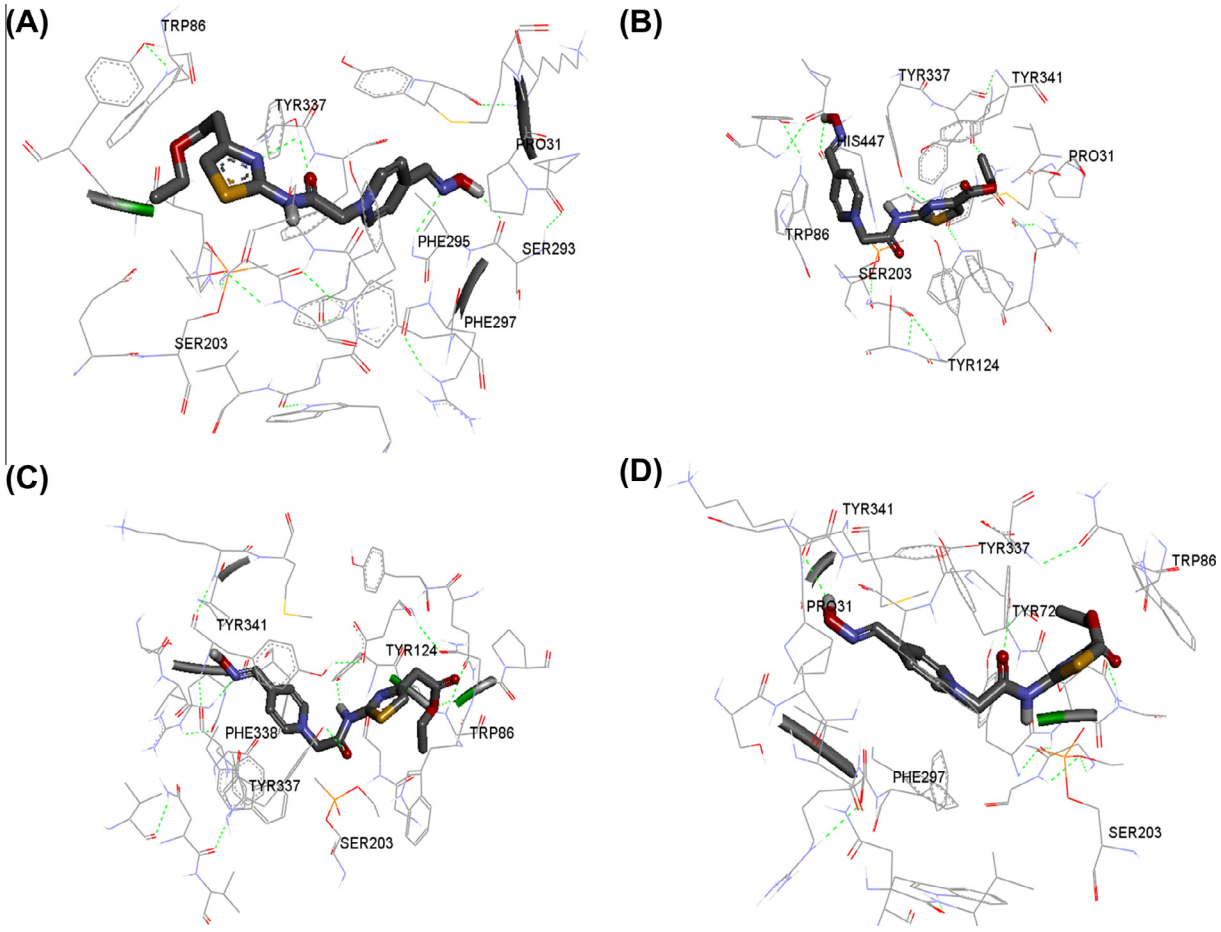

Figure 5. Top-scored docking poses of compounds **5a** and **6a**. (A) Compound **5a** bound to sarin modified *h*AChE; (B) compound **6a** bound to sarin modified *h*AChE; (C) compound **5a** bound to VX/*O*-ethylsarin modified *h*AChE; (D) compound **6a** bound to VX/*O*-ethylsarin modified *h*AChE.

respectively. Further, an additional interaction was observed between TRP 86 and the carboxylic oxygen of the ester group present in the tail of the reactivator (Fig. 5C). Oxime **6a** has H-bonding with the amino acid residues TYR 72 and TYR 341 respectively (Fig. 5D). Compounds **5a** and **6a** have shown comparably similar reactivation efficacies in case of VX and *O*-ethylsarin modified *h*AChE. This was indicated by the close binding energies obtained for both the oximes (Table 2).

Compounds **5a** and **6a** have also shown similar binding energy and reactivation efficacy in case of VX/*O*-ethylsarin modified *h*AChE but different binding energy and reactivation efficacy against sarin inhibited *h*AChE. This may be explained on the basis of their molecular sizes. It is worth mentioned here that VX/*O*-ethyl sarin adduct of SER 203 are smaller in size by one methyl group compared to sarin modified AChE. On the other hand, the oxime **5a** is one methylene group larger than **6a**. Therefore the effect of size of **5a** is marginalized in case of VX/*O*-ethyl sarin but realized in sarin modified *h*AChE. This has been apparent by the reactivation kinetics of both **5a** and **6a**. Overall, oxime **6a** has shown better binding energies with sarin and VX/*O*-ethylsarin modified AChE. This was further reflected by its higher reactivation efficacies against the three tested inhibitors.

Inhibition potency of reactivators is an essential criterion while assessing the efficiency of a drug molecule. Ideally an efficient drug should not affect the native activity of the enzyme. The IC_{50} values were determined for the 4-positioned oximes (**1a**–**6a**) (Table 3) in order to correlate the inhibition potencies of the reactivators with their reactivation efficiencies.

Among the 4-positioned oximes, **5a**, **6a** and **1a** have comparatively lower inhibition potencies as reflected by their higher IC_{50} values. Oximes **2a** and **3a** (0.99 and 0.97 mM) with least IC_{50} values revealed their dominant inhibition character toward the enzyme AChE and this might be responsible for their lower reactivation efficacies than the other tested oximes. In upshot, oximes **5a**, **6a** and **1a** with lower inhibitory activity have demonstrated higher reactivation efficacies against the three OP inhibited AChE (Fig. 6). However, oxime **2a** with higher inhibitory activity was able to reactivate up to 60% of VX, 50% of *O*-ethylsarin and 39% of sarin inhibited human AChE. The overall inhibitory potencies of the tested oximes followed the order: **3a** > **2a** > **4a** > **5a** > **1a** > **6a**.

The dephosphorylation of phosphorylated enzyme is dependent on various factors, such as physicochemical properties, steric and electronic factors, lipophilic–hydrophilic balance and acid dissociation constant (p*K*a) of the reactivator.[9,17] The reactivation of the inhibited AChE is brought about by the attack of a strong

Table 3
IC_{50} values for the oximes **1a**–**6a**

Reactivator	IC_{50} (mM)
1a	2.36
2a	0.99
3a	0.97
4a	1.66
5a	2.27
6a	2.49

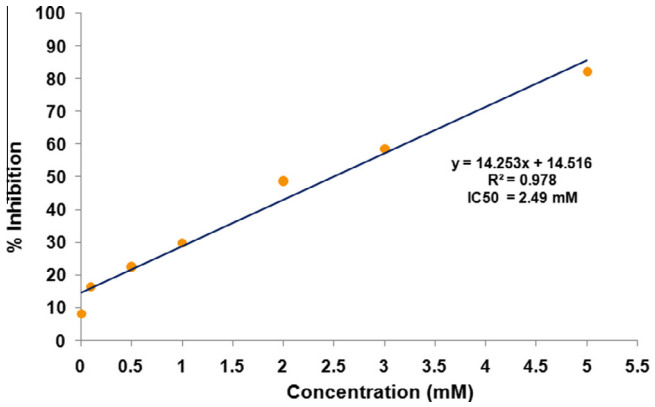

Figure 6. IC_{50} of the oxime **6a**.

nucleophile in order to break the covalent bond formed between the OP and OH group of the serine residue in the catalytic triad of AChE. For this, ionization of oxime into oximate anion is an essential process under the physiological conditions in the reactivation of OP inhibited AChE. Therefore, the p*K*a values should be taken into consideration while searching for new oxime reactivators.[19,56] The determined p*K*a values of all the compounds are given in the Table 4.

It has been observed that the 4-pyridinium oximes have p*K*a in the range of 8–8.5, whereas those of the 3-pyridinium oximes were found in the range of 8.5–8.9. The higher p*K*a values of the 3-pyridinium oximes (**2b**, **3b**, **4b** and **5b**) represented the poorer tendency of the oxime dissociation into the oximate anion. This may be the probable reason that majority of the 3-pyridinium oximes recorded lower reactivation efficacies and lower second order rate constants (k_{r2}) against sarin, *O*-ethylsarin and VX inhibited AChE. All the 4-pyridinium oximes with lower p*K*a values exhibited higher reactivation efficacies. The oximes **5a** (p*K*a: 8.41) and **6a** (p*K*a: 8.31) showed higher reactivation efficacies which were reflected in their higher second order rate constants against VX and *O*-ethylsarin inhibited AChE.

5. Experimental

5.1. Materials and methods

Thiourea, substituted phenacylbromides, 2-aminothiazole, ethyl 4-chloroacetoacetate, ethyl bromopyruvate, 2-, 3- and 4-pyridinealdoxime, acetylthiocholine iodide (ATChI), 5,5′-dithiobis-(2-nitrobenzoic acid) (DTNB), potassium dihydrogenphosphate, dipotassium hydrogenphosphate, trizma-base and trizma-hydrochloride, solvents (isopropanol and *n*-hexane of spectroscopic grade) were purchased from Sigma–Aldrich, USA and used without further purification. Glycine was obtained from E. Merck (India) and used without further purification. Chloroacetyl chloride, anhydrous sodium sulfate, anhydrous sodium bicarbonate and anhydrous potassium carbonate were purchased from Qualigens, India. Solvents (ethanol, dichloromethane, acetonitrile, ethyl acetate, acetone, and methanol) were purchased from SD Fine Chemicals (India) were dried and distilled before use. VX, sarin and *O*-ethylsarin were prepared in this laboratory with >98% purity (GC and ^{31}P NMR). 2-PAM was prepared according to the method of Wilson and Ginsburg.[45] Obidoxime was synthesized using reported methods.[46] All the synthesized compounds as well as standards were characterized by IR, ^{1}H NMR, ^{13}C NMR spectral data and elemental analysis. The progress of reaction and purity of the compounds were checked by thin layer chromatography (TLC) using commercially available pre-coated silica on aluminum sheets purchased from E. Merck, India. The stock solutions of OP inhibitors were prepared in isopropanol and stored at −20 °C. Further dilutions of OP inhibitors were prepared in deionized water. Oxime stock solutions and their further dilutions were prepared freshly in triple distilled water. All the working solutions were kept on ice until the completion of the experiment.

Human blood samples were collected from the volunteers of our laboratory as per norms and the hemoglobin free erythrocyte ghost AChE were prepared using the reported methods.[6,47] The activity of the human AChE was adjusted to that of the whole blood activity and stored at −80 °C until use. Prior to start the inhibition and reactivation experiments, the aliquots of the erythrocyte ghosts were homogenized on ice-bath with the help of an ultrasonic homogenizer (Model 3000, Biologics. Inc., Manassas, USA).

Table 4
Physicochemical data and general chemical structure of the synthesized oximes

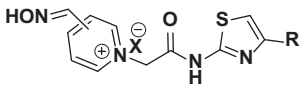

Oxime	Oxime position	X	R	Yield (%)	Mp (°C)	p*K*a
1a	4	Cl	–H	9	216–218	8.39 ± 0.03
1b	3	Cl	–H	17	238–240	8.47 ± 0.04
2a	4	Cl	–Ph-4-H	21	235–237	8.27 ± 0.03
2b	3	I	–Ph-4-H	83	209–211	8.85 ± 0.05
3a	4	Cl	–Ph-4-CH_3	9	220–222	8.38 ± 0.05
3b	3	Cl	–Ph-4-CH_3	6	198–200	8.77 ± 0.04
4a	4	I	–Ph-4-OCH_3	46	218–220	8.54 ± 0.05
4b	3	I	–Ph-4-OCH_3	26	201–203	8.92 ± 0.03
5a	4	Cl	$-CH_2COOC_2H_5$	14	235–237	8.42 ± 0.04
5b	3	Cl	$-CH_2COOC_2H_5$	8	216–218	8.54 ± 0.04
6a	4	Cl	$-COOC_2H_5$	15	243–245	8.32 ± 0.04
6b	3	Cl	$-COOC_2H_5$	19	212–214	8.17 ± 0.04

5.2. Synthesis of monoquaternary pyridinium oximes

A three step simple protocol depicted in Scheme 2 was used to synthesize all the monoquaternary pyridinium oximes (**1a**–**6a** and **1b**–**6b**). The following synthetic procedure described for the compound **2a** was the representative of the whole series.

5.2.1. Synthesis of 4-phenylthiazol-2-amine

Phenacylbromide (5.0 g, 25 mM) and thiourea (1.9 g, 25 mM) were taken in a 50 mL round bottom flask equipped with a condenser, calcium chloride guard tube and magnetic stirrer. The mixture was dissolved in dry ethanol (30 mL) and stirred at room temperature for overnight. Excess solvent was distilled off and the concentrated reaction mixture was slowly poured into a beaker containing ice-cooled saturated sodium bicarbonate solution. The yellow colored precipitate obtained was filtered off, washed thoroughly with chilled water and dried under vacuum (4.2 g, yield: 95%). TLC (ethyl acetate/hexane (1:3), R_f = 0.14). The product obtained was used in the next step without further purification.

5.2.2. Synthesis of 2-chloro-*N*-(4-phenylthiazol-2-yl)acetamide

A suspension of 4-phenylthiazol-2-amine (2 g, 11.4 mM) and anhydrous potassium carbonate (1.89 g, 13.6 mM) in dichloromethane (20 mL) was stirred for 30 min at room temperature. The reaction mixture was then cooled on an ice bath followed by addition of ice-cooled solution of chloroacetyl chloride (1.5 g, 13.6 mM) in dichloromethane (25 mL) in drop wise manner over a period of 30 min. The reaction mixture was then stirred at room temperature overnight followed by reflux for additional 30 min. The excess solvent was distilled off and the residue obtained was neutralized with aqueous sodium bicarbonate solution (5% w/v).

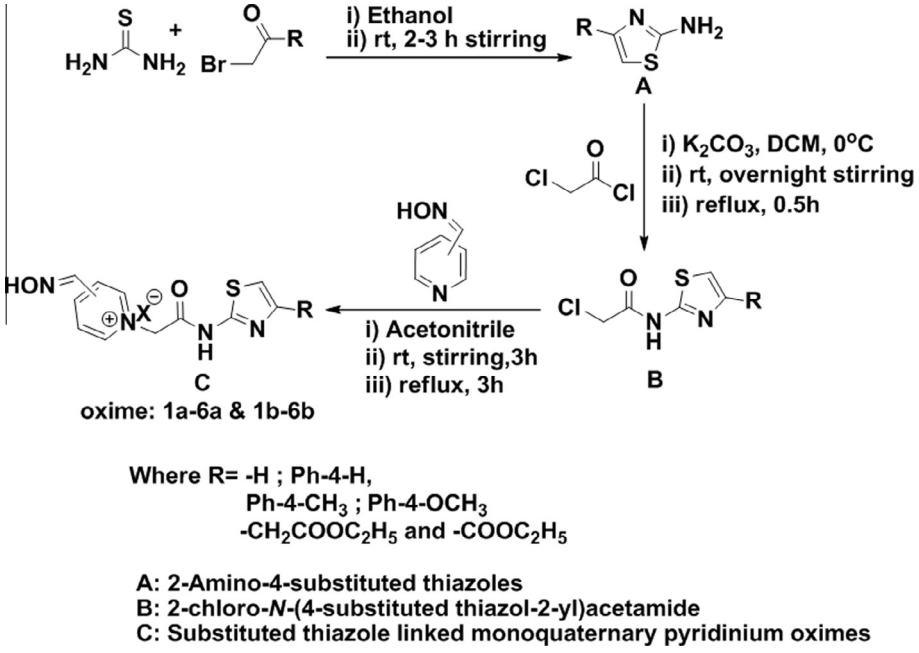

Scheme 2. Synthetic route for the preparation of monoquaternary pyridinium oximes (**1a**–**6a** and **1b**–**6b**).

The solid product formed was filtered off, washed thoroughly with chilled water and dried under vacuum (2.3 g, yield: 80%). TLC (ethyl acetate/hexane (1:3), R_f = 0.31). This product was sufficiently pure and used in the next step without further purification.

5.2.3. Synthesis of 4-((hydroxyiminomethyl)-1-(2-oxo-2-(4-phenylthiazol-2-ylamino)ethyl)pyridinium chloride (2a)

4-Pyridinealdoxime (0.32 g, 2.6 mM), dissolved in dry acetonitrile (25 mL) was taken in a two neck round bottom flask equipped with a magnetic stirrer, condenser and calcium chloride guard tube was stirred at room temperature. 2-Chloro-*N*-(4-phenylthiazol-2-yl)acetamide (0.8 g, 3.2 mM) dissolved in dry acetonitrile (20 mL) was added to the reaction mixture slowly over a period of 10 min. The reaction mixture was then stirred for 3 h at room temperature followed by reflux for another 3 h. The solid product obtained was filtered off, washed with dry hot acetonitrile (3 × 15 mL) followed by dry hot acetone. The crude product was dried (0.88 g, yield: 75%) and recrystallized from methanol-acetone mixture. TLC (acetone/methanol (2:1), R_f = 0.10), mp: 235–237 °C.

Note: The iodo variants (**2b**, **4a** and **4b**) of compound **B** in Scheme 2 were prepared by exchanging the chloro group with iodide using sodium iodide, by refluxing in dry acetone.

Except **1a** and **1b**, all other compounds were prepared by following the same protocol as mentioned above while **1a** and **1b** were prepared directly from the second step of the above protocol. Melting points were determined with open capillary in conventional method and were uncorrected (Table 4).

Elemental analyses were conducted on an ELEMENTAR, vario MICRO cube, Universal micro analyzer and the values were within ±0.4% of the calculated values. Infra-red (IR) spectra were obtained from KBr disks on a Bruker TENSOR-27 FTIR spectrophotometer. ^{1}H NMR (DMSO-d_6) spectra of the synthesized oximes were recorded on Bruker Avance 400 spectrometer at 400 MHz using tetramethylsilane (TMS) as internal standard and expressed in the δ (ppm) values. ^{13}C NMR (DMSO-d_6) chemical shifts values were obtained using the same instrument at 100 MHz.

5.3. Spectroscopic data for the synthesized oximes

5.3.1. 4-((Hydroxyimino)methyl)-1-(2-oxo-2-(thiazol-2-ylamino)ethyl)pyridinium chloride (1a)

Creamish powder; IR (KBr) ν_{max} 3053, 3046, 2957, 1687, 1640, 1592, 1461, 1322 cm^{-1}; ^{1}H NMR (DMSO-d_6, 400 MHz): δ (ppm) = 5.756 (s, 2H, –NCH_2), 7.296 (d, 1H, J = 3.6 Hz, =CH–S), 7.524 (d, 1H, J = 3.6 Hz, =CH–N), 8.299 (d, 1H, J = 6.8 Hz, –Py), 8.456 (s, 1H, –CH=N), 9.02 (d, 2H, J = 6.8 Hz, –Py), 12.992 (s, 1H, –OH); ^{13}C NMR (DMSO-d_6, 100 MHz): δ (ppm) = 61.2, 114.1, 123.4, 129.2, 144.9, 146.6, 149.2, 157.1, 168.2; Anal. Calcd for $C_{11}H_{11}ClN_4O_2S$: C, 44.22; H, 3.71; N, 18.75; S, 10.73. Found: C, 44.64; H, 4.06; N, 18.34; S, 10.31.

5.3.2. 3-((Hydroxyimino)methyl)-1-(2-oxo-2-(thiazol-2-ylamino)ethyl)pyridinium chloride (1b)

Off-white powder; IR (KBr) ν_{max} 3191, 3070, 3015, 1683, 1629, 1582, 1469, 1326 cm^{-1}; ^{1}H NMR (DMSO-d_6, 400 MHz): δ (ppm) = 5.851 (s, 2H, –NCH_2), 7.296 (d, 1H, J = 3.6 Hz, =CH–S), 7.52 (d, 1H, J = 3.2 Hz, =CH–N), 8.245 (dd, 1H, J = 6.0 Hz & 2.0 Hz, –Py), 8.376 (s, 1H, –CH=N), 8.808 (d, 1H, J = 8.4 Hz, –Py), 9.079 (d, 1H, J = 6.0 Hz, –Py), 9.349 (s, 1H, –Py), 12.363 (s, 1H, –NH), 12.979 (s, 1H, –OH); ^{13}C NMR (DMSO-d_6, 100 MHz): δ (ppm) = 61.9, 114.1, 127.6, 133.0, 142.6, 143.0, 143.8, 145.9, 159.1, 168.3; Anal. Calcd for $C_{11}H_{11}ClN_4O_2S$: C, 44.22; H, 3.71; N, 18.75; S, 10.73. Found: C, 43.94; H, 3.67; N, 18.46; S, 10.40.

5.3.3. 4-((Hydroxyimino)methyl)-1-(2-oxo-2-(4-phenylthiazol-2-ylamino)ethyl)pyridinium chloride (2a)

Pale yellow powder; IR (KBr) ν_{max} 3117, 3022, 2944, 1694, 1642, 1610, 1469, 1350 cm^{-1}; ^{1}H NMR (DMSO-d_6, 400 MHz): δ (ppm) = 5.818 (s, 2H, –NCH_2), 7.346 (t, 2H, J = 7.6 Hz, –Ph), 7.45 (t, 2H, J = 7.6 Hz, –Ph), 7.717 (s, 1H, =CH–S), 7.916 (d, 2H, J = 7.6 Hz, –Ph), 8.316 (d, 1H, J = 6.4 Hz, –Py), 8.466 (s, 1H, –CH=N), 9.06 (d, 2H, J = 6.4 Hz, –Py), 13.017 (s, 1H, –NH), 13.108 (s, 1H, –OH); ^{13}C NMR (DMSO-d_6, 100 MHz): δ (ppm) = 61.1, 108.7, 123.5, 125.7, 127.9, 128.7, 133.9, 144.9, 146.7, 149.1, 149.3, 157.1, 164.3; Anal. Calcd for $C_{17}H_{15}ClN_4O_2S$: C, 54.47; H, 4.03; N, 14.95; S, 8.55. Found: C, 54.09; H, 4.26; N, 14.89; S, 8.21.

5.3.4. 3-((Hydroxyimino)methyl)-1-(2-oxo-2-(4-phenylthiazol-2-ylamino)ethyl)pyridinium chloride (2b)

Creamish powder; IR (KBr) ν_{max} 3108, 3076, 2966, 1688, 1634, 1599, 1501, 1344 cm^{-1}; ^1H NMR (DMSO-d_6, 400 MHz): δ (ppm) = 5.810 (s, 2H, –NCH_2), 7.350 (t, 2H, J = 7.2 Hz, –Ph), 7.455 (t, 2H, J = 7.6 Hz, –Ph), 7.722 (s, 1H, =CH–S), 7.915 (d, 2H, J = 7.6 Hz, –Ph), 8.267 (dd, 1H, J = 6.4 Hz & 1.6 Hz, –Py), 8.393 (s, 1H, –CH=N), 8.82 (d, 1H, J = 8.0 Hz, –Py), 9.032 (d, 1H, J = 6.0 Hz, –Py), 9.322 (s, 1H, –Py), 12.317 (s, 1H, –NH), 13.110 (s, 1H, –OH); ^{13}C NMR (DMSO-d_6, 100 MHz): δ (ppm) = 61.8, 108.7, 125.6, 127.6, 127.9, 128.7, 132.9, 133.9, 142.9, 143.2, 143.8, 145.9, 163.8; Anal. Calcd for $C_{17}H_{15}ClN_4O_2S$: C, 54.47; H, 4.03; N, 14.95; S, 8.55. Found: C, 54.87; H, 4.03; N, 14.91; S, 8.83.

5.3.5. 4-((Hydroxyimino)methyl)-1-(2-oxo-2-(4-p-tolylthiazol-2-ylamino)ethyl)pyridinium chloride (3a)

Tan powder; IR (KBr) ν_{max} 3108, 3029, 2914, 1694, 1644, 1567, 1467, 1322 cm^{-1}; ^1H NMR (DMSO-d_6, 400 MHz): δ (ppm) = 2.333 (s, 3H, –CH_3), 5.789 (s, 2H, –NCH_2), 7.254 (d, 2H, J = 8.0 Hz, –Ph), 7.627 (s, 1H, =CH–S), 7.799 (d, 2H, J = 8.0 Hz, –Ph), 8.311 (d, 1H, J = 6.4 Hz, –Py), 8.463 (s, 1H, –CH=N), 9.041 (d, 2H, J = 6.4 Hz, –Py), 12.995 (s, 1H, –OH); ^{13}C NMR (DMSO-d_6, 100 MHz): δ (ppm) = 20.7, 107.8, 123.4, 125.6, 129.2, 130.3, 136.8, 137.2, 145.0, 146.6, 149.2, 150.2, 164.1, 169.2; Anal. Calcd for $C_{18}H_{17}ClN_4O_2S$: C, 55.59; H, 4.41; N, 14.41; S, 8.25. Found: C, 55.91; H, 4.41; N, 14.74; S, 8.58.

5.3.6. 3-((Hydroxyimino)methyl)-1-(2-oxo-2-(4-p-tolylthiazol-2-ylamino)ethyl)pyridinium chloride (3b)

Tan powder; IR (KBr) ν_{max} 3137, 3046, 2951, 1700, 1634, 1556, 1428, 1300 cm^{-1}; ^1H NMR (DMSO-d_6, 400 MHz): δ (ppm) = 2.336 (s, 3H, –CH_3), 5.820 (s, 2H, –NCH_2), 7.257 (d, 2H, J = 8.0 Hz, –Ph), 7.632 (s, 1H, =CH–S), 7.80 (d, 2H, J = 8.0 Hz, –Ph), 8.254 (m, 1H, –Py), 8.385 (s, 1H, –CH=N), 8.811 (d, 1H, J = 8.0 Hz, –Py), 9.043 (d, 1H, J = 6.0 Hz, –Py), 9.328 (s, 1H, –Py), 12.297 (s, 1H, –NH), 13.019 (s, 1H, –OH); Anal. Calcd for $C_{18}H_{17}ClN_4O_2S$: C, 55.59; H, 4.41; N, 14.41; S, 8.25. Found: C, 55.25; H, 4.43; N, 14.46; S, 8.66.

5.3.7. 4-((Hydroxyimino)methyl)-1-(2-(4-(4-methoxyphenyl) thiazol-2-ylamino)-2-oxoethyl)pyridinium chloride (4a)

Yellow powder; IR (KBr) ν_{max} 3117, 3026, 2957, 1705, 1642, 1605, 1488, 1324 cm^{-1}; ^1H NMR (DMSO-d_6, 400 MHz): δ (ppm) = 3.798 (s, 3H, –OCH_3), 5.722 (s, 2H, –NCH_2), 7.009 (d, 2H, J = 8.8 Hz, –Ph), 7.541 (s, 1H, =CH–S), 7.84 (d, 2H, J = 8.8 Hz, –Ph), 8.31 (d, 1H, J = 6.4 Hz, –Py), 8.462 (s, 1H, –CH=N), 8.99 (d, 2H, J = 6.4 Hz, –Py), 12.924 (s, 1H, –OH); ^{13}C NMR (DMSO-d_6, 100 MHz): δ (ppm) = 55.7, 61.1, 103.1, 107.2, 114.6, 124.0, 127.5, 140.1, 145.6, 147.1, 149.7, 157.5, 159.6, 164.5; Anal. Calcd for $C_{18}H_{17}ClN_4O_3S$: C, 53.40; H, 4.23; N, 13.84; S, 7.92. Found: C, 55.37; H, 4.11; N, 13.84; S, 7.49.

5.3.8. 3-((Hydroxyimino)methyl)-1-(2-(4-(4-methoxyphenyl) thiazol-2-ylamino)-2-oxoethyl)pyridinium chloride (4b)

Pale yellow powder; IR (KBr) ν_{max} 3191, 3074, 2988, 1700, 1631, 1607, 1488, 1318 cm^{-1}; ^1H NMR (DMSO-d_6, 400 MHz): δ (ppm) = 3.798 (s, 3H, –OCH_3), 5.784 (s, 2H, –NCH_2), 7.009 (d, 2H, J = 8.8 Hz, –Ph),7.544 (s, 1H, =CH–S), 7.841 (d, 2H, J = 8.8 Hz, –Ph), 8.386 (s, 1H, –CH=N), 9.014 (d, 1H, J = 6.4 Hz, –Py), 9.304 (s, 1H, –Py), 12.265 (s, 1H, –NH), 12.951 (s, 1H, –OH); ^{13}C NMR (DMSO-d_6, 100 MHz): δ (ppm) = 55.1, 61.8, 106.6, 114.1, 126.7, 127.0, 127.6, 132.9, 142.9, 143.2, 143.8, 145.9, 159.1, 163.8, 167.2; Anal. Calcd for $C_{18}H_{17}ClN_4O_3S$: C, 53.40; H, 4.23; N, 13.84; S, 7.92. Found: C, 53.05; H, 4.55; N, 13.91; S, 7.56.

5.3.9. 1-(2-(4-(2-Ethoxy-2-oxoethyl)thiazol-2-ylamino)-2-oxoethyl)-4-((hydroxyimino)methyl)pyridinium chloride (5a)

White powder; IR (KBr) ν_{max} 3115, 3085, 2981, 1739, 1694, 1644, 1556, 1469, 1298 cm^{-1}; ^1H NMR (DMSO-d_6, 400 MHz): δ (ppm) = 1.186 (t, 3H, J = 7.2 Hz, –CH_3), 3.716 (s, 2H, –CH_2), 4.087 (q, 2H, J = 7.2 Hz, –CH_2), 5.737 (s, 2H, –NCH_2), 7.071 (s, 1H, =CH–S), 8.30 (d, 2H, J = 6.8 Hz, –Py), 8.455 (s, 1H, –CH=N), 9.011 (d, 2H, J = 6.8 Hz, –Py), 12.951 (s, 1H, –NH), 12.988 (s, 1H, –OH); ^{13}C NMR (DMSO-d_6, 100 MHz): δ (ppm) = 14.0, 36.5, 60.2, 61.0, 111.1, 123.4, 144.9, 146.6, 149.2, 156.2, 159.2, 168.7, 169.8; Anal. Calcd for $C_{15}H_{17}ClN_4O_4S$: C, 46.81; H, 4.45; N, 14.56; S, 8.33. Found: C, 46.46; H, 4.39; N, 14.56; S, 8.12.

5.3.10. 1-(2-(4-(2-Ethoxy-2-oxoethyl)thiazol-2-ylamino)-2-oxoethyl)-3-((hydroxyimino)methyl)pyridinium chloride (5b)

Off-white powder; IR (KBr) ν_{max} 3124, 3031, 2994, 1731, 1696, 1635, 1558, 1471, 1341 cm^{-1}; ^1H NMR (DMSO-d_6, 400 MHz): δ (ppm) = 1.186 (m, 3H, –CH_3), 3.717 (s, 2H, –CH_2), 4.088 (q, 2H, J = 7.2 Hz, –CH_2), 5.792 (s, 2H, –NCH_2), 7.072 (s, 1H, =CH–S), 8.242 (dd, 1H, J = 6.0 Hz & 2.0 Hz, –Py), 8.374 (s, 1H, –CH=N), 8.80 (d, 1H, J = 8.0 Hz, –Py), 9.036 (d, 1H, J = 6.0 Hz, –Py), 9.319 (s, 1H, –Py), 12.320 (s, 1H, –NH), 12.944 (s, 1H, –OH); ^{13}C NMR (DMSO-d_6, 100 MHz): δ (ppm) = 14.0, 40.1, 60.2, 61.7, 111.1, 127.6, 133.0, 142.7, 143.0, 143.8, 145.9, 152.9, 158.7, 162.3, 169.8; Anal. Calcd for $C_{15}H_{17}ClN_4O_4S$: C, 46.81; H, 4.45; N, 14.56; S, 8.33. Found: C, 46.09; H, 4.38; N, 14.45; S, 8.09.

5.3.11. 1-(2-(4-(Ethoxycarbonyl)thiazol-2-ylamino)-2-oxoethyl)-4-((hydroxyimino)methyl)pyridinium chloride (6a)

White powder; IR (KBr) ν_{max} 3119, 3042, 2983, 1726, 1698, 1642, 1610, 1463, 1290 cm^{-1}; ^1H NMR (DMSO-d_6, 400 MHz): δ (ppm) = 1.301 (m, 3H, –CH_3), 4.287 (q, 2H, J = 7.2 Hz, –CH_2), 5.750 (s, 2H, –NCH_2), 8.129 (s, 1H, =CH–S), 8.303 (d, 2H, J = 6.8 Hz, –Py), 8.454 (s, 1H, –CH=N), 8.999 (d, 2H, J = 6.8 Hz, –Py), 12.968 (s, 1H, –NH), 13.306 (s, 1H, –OH); ^{13}C NMR (DMSO-d_6, 100 MHz): δ (ppm) = 14.1, 24.8, 60.6, 61.0, 123.3, 123.4, 141.1, 145.0, 146.6, 149.3, 157.3, 160.7, 164.7; Anal. Calcd for $C_{14}H_{15}ClN_4O_4S$: C, 45.35; H, 4.08; N, 15.11; S, 8.65. Found: C, 45.17; H, 4.03; N, 15.16; S, 8.52.

5.3.12. 1-(2-(4-(Ethoxycarbonyl)thiazol-2-ylamino)-2-oxoethyl)-3-((hydroxyimino)methyl)pyridinium chloride (6b)

Creamish powder; IR (KBr) ν_{max} 3139, 3089, 2985, 1727, 1696, 1638, 1556, 1465, 1285 cm^{-1}; ^1H NMR (DMSO-d_6, 400 MHz): δ (ppm) = 1.302 (t, 3H, J = 7.2 Hz, –CH_3), 4.287 (q, 2H, J = 7.2 Hz, –CH_2), 5.795 (s, 2H, –NCH_2), 8.127 (s, 1H, =CH–S), 8.248 (dd, 1H, J = 6.4 Hz & 1.6 Hz, –Py), 8.376 (s, 1H, –CH=N), 8.803 (d, 1H, J = 8.0 Hz, –Py), 9.017 (d, 1H, J = 6.4 Hz, –Py), 9.307 (s, 1H, –Py), 12.293 (s, 1H, –NH), 12.850 (s, 1H, –OH); Anal. Calcd for $C_{14}H_{15}ClN_4O_4S$: C, 45.35; H, 4.08; N, 15.11; S, 8.65. Found: C, 45.55; H, 4.29; N, 15.46; S, 8.31.

5.4. AChE assay

AChE activities were measured at 412 nm by using UV-Visible spectrophotometer (Cary 100, Agilent Technologies, USA) assisted with PCB 1500 water Peltier system with a modified Ellman protocol.[48–50] Quartz cuvettes of 3 mL were used to measure the activity of the assay mixture. ATChI (0.48 mM, in distilled water) as substrate and DTNB as the colorimetric indicator (0.3 mM in 0.1 M phosphate buffer, pH = 7.4) were used to assay the activity. All experiments were performed at 37 °C in phosphate buffer at pH 7.4. All concentrations in the above assay mixture refer to the final concentrations.

5.5. AChE inhibition by OP

The initial stock solutions of OP inhibitors (sarin, *O*-ethylsarin and VX) were prepared in isopropanol and stored in refrigerator. Subsequent dilutions of OP inhibitors were freshly prepared in deionized water prior to start the experiment. The enzyme *h*AChE was taken in phosphate buffer (pH 7.4, 0.1 M) was inhibited by appropriate OP concentrations at 37 °C for 10–15 min to achieve 95–98% inhibition of the control activity. Excess OP nerve agent was removed by extraction of the inhibition cocktail with six fold volume of *n*-hexane.[51,52]

5.6. Oxime assisted reactivation kinetics of OP inhibited *h*AChE

The OP inhibited *h*AChE was subjected to the reactivation by the addition of the synthesized oximes at final concentrations ranging from 10 to 1000 μM. Five different oxime concentrations (10, 50, 100, 500 and 1000 μM) were used for the determination of rate constants at different time points (1, 3, 5, 7, 10, 15, 20 25, 30, 40, 50, 60 min). An aliquot of 50 μL from the reactivation cocktail (containing inhibition cocktail and oxime reactivator) was transferred to the cuvette containing 3.0 mL of phosphate buffer and 100 μL of DTNB. Shortly afterward the AChE activity was assayed by adding 20 μL of ATChI at 37 °C (final volume 3.17 mL). The oxime induced reactivation of the OP-inhibited AChE was monitored at different time intervals over a period of 60 min. Spontaneous reactivation of inhibited AChE was assayed using the same protocol (the reaction mixture containing enzyme and OP but no oxime). Under these conditions spontaneous reactivation was found to be insignificant. All the values were corrected for their oxime induced hydrolysis of ATChI.

The oxime assisted reactivation of the OP-inhibited AChE proceeds according to the Scheme 3.

Where [EP] phosphylated AChE; [OX] the reactivator; [EPOX] reversible Michaelis-type phosphyl–AChE–oxime complex; [E] reactivated enzyme and [POX] phosphylated oxime. [EP]*[OX]/[EPOX] estimates the dissociation constant (K_D) and inversely proportional to the affinity of the oxime to [EP]. k_r represents the rate constant for the displacement of the phosphyl residue from [EPOX] by the oxime and indicates the reactivation potency of the oxime reactivator.

In case of complete reactivation and with [OX] ≫ $[EP]_o$ a pseudo first-order rate equation can be derived for the reactivation process as represented in Eq. 1

$$k_{obs} = \frac{k_r[OX]}{K_D + [OX]} \quad (1)$$

where k_{obs} is the observed first-order rate constant of the reactivation at any given oxime concentration and it was calculated by non-linear regression analysis[6] using Eq. 2

$$v_t = v_o \times (1 - e^{-k_{obs} \times t}) \quad (2)$$

k_r and K_D were obtained by the non-linear fit of the relationship between k_{obs} versus [OX]. Both the rate constants k_r and K_D follow Michaelis–Menten type kinetics and the second order reactivation rate constant k_{r2} was obtained from the ratio of k_r and K_D.

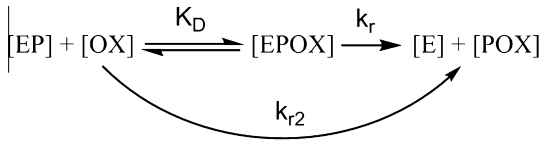

Scheme 3. Oxime assisted reactivation of OP-inhibited AChE.

The determined kinetic parameters and rate constants of all the oximes were presented in the Table 1.

5.7. Data analysis

The kinetic rate constants were determined by processing the experimental data with non-linear regression analysis using curve fitting programs provided by Prism™ Vers. 6.0 (Graph Pad software, San Diego, USA).

5.8. Docking simulations

Simulation for receptor—ligand docking was carried out on Auto Dock 4.0 (Sanner, 1999)[53] using a reported method with slight modification (Musilek et al., 2011).[24] Briefly, structure of human AChE (PDB–ID 1B41) was obtained from the protein data bank and used in docking studies. After eliminating the inhibitor 'Fasciculin-2' and water molecules, SER 203 was modified with sarin and VX reaction products, respectively. *O*-Ethylsarin reaction product was same as VX reaction product. Oximes were drawn, energy minimized and prepared as ligands. Pre-calculated electrostatic grid map for each atom type present in ligands were generated. All maps were created with 0.375 Å spacing and the γ-oxygen atom of SER 203 was selected as grid center. The dimension of grid box was set at 60 Å × 60 Å × 60 Å, the accessible space for ligand around grid center. Docking calculations were carried out using Lamarckian genetic algorithm (LGA). A population of 150 random individuals, a maximum of 2,500,000 energy evaluations, a maximum of 27,000 generations, maximum 1 top individual surviving, 0.02 rate of gene mutation and 0.8 rate of crossover were used as parameters for LGA. At the end of docking, the resulting positions (10 runs) were clustered according to root mean square criterion of 0.5 Å.

5.9. Determination of acid dissociation constant (p*K*a)

5.9.1. Reagents

Oxime stock solutions (5×10^{-3} M) were freshly prepared in triple distilled water. Buffer solutions were prepared from the methods reported in literature (Gomori, 1955).[54] The analytical wavelengths for the protonated and deprotonated species were obtained by using 0.1 M hydrochloric acid and 0.1 M sodium hydroxide solutions.

The acid dissociation constants (p*K*a) of the oximes were determined using the method of Albert and Sergeant (1971).[55,56] The method was based on direct determination of the ratio of molecular species (protonated) to dissociated (deprotonated) species in a series of non-absorbing buffer solutions. For this purpose, spectra of molecular species were obtained first in buffer solution of particular pH in which compounds of interest would be present entirely in either form. Oxime stock solutions (15–35 μL, 5×10^{-3} M) were diluted to 3 mL in a cuvette containing either 0.1 M hydrochloric acid or 0.1 M sodium hydroxide solution and the absorption spectra of oxime in acid or alkali were recorded over the wavelength range of 200–600 nm with a reference blank solution at 25 ± 1.0 °C. The spectra, thus obtained in acid or alkali, were of protonated (D_m) and deprotonated (D_i) molecules (Fig. 7). Eleven different pH values, ranging from 6.85 to 9.76 were selected to determine the p*K*a of oximes. For this, appropriate buffers consisting of phosphate (pH: 6.85–7.76), tris (pH: 8.17–8.56) and glycine-NaOH (pH: 9.03–9.76) were used to determine the dissociation constants of oximes. 15–35 μL of aqueous solutions of oximes were diluted to 3 mL in each buffer and optical densities were determined at analytical wavelengths using buffer blank at 25 ± 1.0 °C. A set of eleven values of p*K*a were obtained using the following Eq. 3:

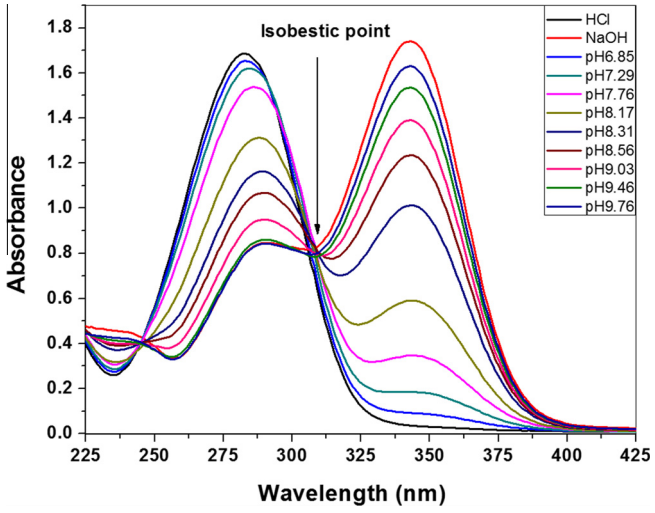

Figure 7. Spectrophotometric determination of p*K*a of the oxime **1a**.

$$pKa = pH + \log[(D_i - D)/(D - D_m)] \quad (3)$$

where, D_m and D_i corresponds to the optical density of protonated and deprotonated forms of the oxime, and D is the optical density in the buffer. The average value of the eleven measurements was considered as the p*K*a of the compound with respect to oximino functionality (Table 4). UV–Visible spectrophotometer (Cary 100, Agilent Technologies, USA) assisted with water Peltier system was used for spectrophotometric analysis. The pH values of the buffer solutions were determined by using Eutech 1500 Cyberscan pH meter. The pH meter was calibrated at 25 °C with standard buffer solutions pH 7.00 and 9.21.

6. Conclusion

In the present investigation, the synthesized thiazole linked mono-pyridinium oximes were evaluated for their in vitro reactivation efficacy against sarin, *O*-ethylsarin and VX inhibited human AChE. Oximes having conformationally flexible aliphatic ester linkers were identified as potential reactivators than their aromatic counterparts. Compounds 1-(2-(4-(2-ethoxy-2-oxoethyl)thiazol-2-ylamino)-2-oxoethyl)-4-((hydroxyimino)methyl)pyridinium chloride (**5a**), 1-(2-(4-(ethoxycarbonyl)thiazol-2-ylamino)-2-oxoethyl)-4-((hydroxyimino)methyl)pyridinium chloride (**6a**) and 4-((hydroxyimino)methyl)-1-(2-oxo-2-(thiazol-2-ylamino)ethyl)pyridinium chloride (**1a**) have shown superior reactivation ability among all the tested oximes. The in vitro reactivation study supports the fact that the position of the oxime group plays vital role in the assessment of the antidotal efficacies. Further, the oximes **5a** and **6a** were subjected to molecular docking studies which revealed the favorable orientations of the reactivator in the active site of the enzyme. In addition, the docking studies clearly demonstrated the importance of the H-bonding interactions in the assessment of the reactivation efficacy of the newly synthesized molecules. It was evident from this study that the reactivation of OP inhibited AChE not only relies on the structure and position of the reactivator but also on the structure of the inhibitor and the behavior of the tetrahedral OP–AChE complex inside the gorge.

Acknowledgements

Authors are thankful to the Director, Defence Research and Development Establishment (DRDE), Gwalior for his keen interest in this work. Authors are also highly thankful to Prof. Franz Worek, Bundeswehr Institute of Pharmacology and Toxicology, Munich, Germany, for his valuable suggestions during optimization of the experimental protocol. Authors highly appreciate the help of the Microbiology, Biotechnology and Biochemistry Divisions, of DRDE, Gwalior for their help and technical support in the isolation of human AChE. Authors are thankful to Mr. Ajay Pratap for spectral characterization of the synthesized compounds. Authors are thankful to Prof. K. K. Ghosh, PRSU, Raipur for his kind help in the calculation of kinetic rate constants. Aditya Kapil Valiveti is thankful to Defence Research & Development Organization (DRDO), New Delhi for financial support.

References and notes

1. Schrader, G. *Angew. Chem.* **1961**, *73*, 331.
2. Enserink, M. *Science* **2013**, *341*, 1050.
3. Masuda, N.; Takatsu, M.; Morinari, H.; Ozawa, T.; Nozaki, H.; Aikawa, N. *Lancet* **1995**, *345*, 1446.
4. Eddleston, M.; Eyer, P.; Worek, F.; Mohamed, F.; Senarathna, L.; von Meyer, L.; Juszczak, E.; Hittarage, A.; Azhar, S.; Dissanayake, W.; Sheriff, R. M. H.; Szinicz, L.; Dawson, H. A.; Buckley, A. N. *Lancet* **2005**, *366*, 1452.
5. Koelle, G. B. *Cholinesterases and Anticholinesterase Agents*; Springer-Verlag: Berlin, 1976. p 123.
6. Worek, F.; Thiermann, H.; Szinicz, L.; Eyer, P. *Biochem. Pharmacol.* **2004**, *68*, 2237.
7. Jokanovic, M. *Toxicology* **2001**, *166*, 139.
8. Skrinjaric-Spoljar, M.; Simeon, V.; Reiner, E. *Biochim. Et. Biophys. Acta. (BBA)—Enzymol.* **1973**, *315*, 363.
9. Gray, A. P. *Drug Metab. Rev.* **1984**, *15*, 557.
10. Thiermann, H.; Worek, F.; Szinicz, L. *J. Toxicol. Clin. Toxicol.* **2003**, *41*, 457.
11. Heath, A. J. W.; Meredith, T. Atropine in the Management of Anticholinesterase Poisoning. In *Clinical and Experimental Toxicology of Organophosphates and Carbamates*; Ballantyne, B., Marrs, T. C., Eds.; Butterworth Heinemann: Oxford, 1992; p 543.
12. Worek, F.; Widmann, R.; Knopff, O.; Szinicz, L. *Arch. Toxicol.* **1998**, *72*, 237.
13. Jokanovic, M.; Maksimovic, M. *Arch. Toxicol.* **1995**, *70*, 119.
14. Lorke, D. E.; Kalasz, H.; Petroianu, G. A.; Tekes, K. *Curr. Med. Chem.* **2008**, *15*, 743.
15. Chambers, J. E.; Chambers, H. W.; Meek, E. C.; Pringle, R. B. *Chemi. Biol. Interact.* **2013**, *203*, 135.
16. Antonijevic, B.; Stojiljkovic, M. *Clin. Med. Res.* **2007**, *5*, 71.
17. Voicu, V. A.; Thiermann, H.; Radulescu, S. F.; Mircioiu, C.; Miron, S. D. *Basic Clin. Pharmacol. Toxicol.* **2009**, *106*, 73.
18. Mercey, G.; Verdelet, T.; Renou, J.; Kliachyna, M.; Baati, R.; Nachon, F.; Jean, L.; Renard, P. Y. *Acc. Chem. Res.* **2012**, *45*, 756.
19. Acharya, J.; Rana, H.; Valiveti, A. K.; Kaushik, M. P. *Med. Chem. Res.* **2013**, *22*, 1277.
20. Bharate, S. B.; Guo, L.; Reeves, T. E.; Cerasoli, D. M.; Thompson, C. M. *Bioorg. Med. Chem. Lett.* **2009**, *19*, 5101.
21. (a) Karade, H. N.; Valiveti, A. K.; Acharya, J.; Kaushik, M. P. *Bioorg. Med. Chem.* **2014**, *22*, 2684; (b) Kumar, P.; Swami, D.; Karade, H. N.; Acharya, J.; Jatav, P. C.; Kumar, A.; Meena, M. K. *Cell Mol. Biol.* **2014**, *60*, 53.
22. Kuca, K.; Cabal, J.; Jun, D.; Hrabinova, M. *Drug Chem. Toxicol.* **2006**, *29*, 443.
23. Musilek, K.; Holas, O.; Misik, J.; Pohanka, M.; Novotny, L.; Dohnal, V.; Opletalova, V.; Kuca, K. *ChemMedChem* **2010**, *5*, 247.
24. Musilek, K.; Komloova, M.; Holas, O.; Horova, A.; Pohanka, M.; Gunn-Moore, F.; Dohnal, V.; Dolezal, M.; Kuca, K. *Bioorg. Med. Chem.* **2011**, *19*, 754.
25. Musilek, K.; Holas, O.; Jun, D.; Dohnal, V.; Gunn-Moore, F.; Opletalova, V.; Dolezal, M.; Kuca, K. *Bioorg. Med. Chem.* **2007**, *15*, 6733.
26. Odzak, R.; Calic, M.; Hrenar, T.; Primozic, I.; Kovarik, Z. *Toxicology* **2007**, *233*, 85.
27. Sit, R. K.; Fokin, V. V.; Amitai, G.; Sharpless, K. B.; Taylor, P.; Radic, Z. *J. Med. Chem.* **2014**, *57*, 1378.
28. Luo, C.; Tong, M.; Chilukuri, N.; Brecht, K.; Maxwell, D. M.; Saxena, A. *Biochemistry* **2007**, *46*, 11771.
29. Worek, F.; Reiter, G.; Eyer, P.; Szinicz, L. *Arch. Toxicol.* **2002**, *76*, 523.
30. Gray, P. J.; Dawson, R. M. *Toxicol. Appl. Pharmacol.* **1987**, *91*, 140.
31. Szinicz, L.; Worek, F.; Thiermann, H.; Kehe, K.; Eckert, S.; Eyer, P.; Eyer, P. *Toxicology* **2007**, *233*, 23.
32. Worek, F.; Thiermann, H. *Pharmacol. Ther.* **2013**, *139*, 249.
33. Bachir, M.; Riffaud, J. P.; Lacolle, J. Y.; Lemoine, J.; Almeida, A. D.; Houziaux, P.; Danree, B. *Eur. J. Med. Chem.* **1990**, *25*, 71.
34. Parmar, K. A.; Suthar, B. G.; Parajapati, S. *Bull. Korean Chem. Soc.* **2010**, *31*, 793.
35. Wauquier, A.; Clincke, C.; Ashton, D.; DeRyck, M.; Fransen, J.; Van Clemen, G. *Drug Dev. Res.* **1986**, *8*, 373.
36. Laras, Y.; Quéléver, G.; Garino, Ć.; Pietrancosta, N.; Sheha, M.; Bihel, F.; Wolfe, M. S.; Kraus, J. L. *Org. Biomol. Chem.* **2005**, *3*, 612.
37. Lee, Y. S.; Kim, H.; Kim, Y. H.; Roh, E. J.; Han, H.; Shin, K. J. *Bioorg. Med. Chem. Lett.* **2012**, *22*, 7555.
38. Martinez, G. et al. US Patent No: **2009**/0221647 A1.
39. Bulic, B.; Pickhardt, M.; Mandelkow, E. M.; Mandelkow, E. *Neuropharmacology* **2010**, *59*, 276.
40. Gallivan, J. P.; Dougherty, D. A. *Proc. Natl. Acad. Sci. U.S.A.* **1999**, *96*, 9459.

41. Sussman, J. L.; Harel, M.; Frolow, F.; Oefner, C.; Goldman, A.; Toker, L. *Science* **1991**, *253*, 872.
42. Worek, F.; Eyer, P.; Aurbek, N.; Szinicz, L.; Thiermann, H. *Toxicol. Appl. Pharmacol.* **2007**, *219*, 226.
43. Forsberg, A.; Puu, G. *Eur. J. Biochem.* **1984**, *140*, 153.
44. Maxwell, D. M.; Koplovitz, I.; Worek, F.; Sweeney, R. E. *Appl. Pharmacol.* **2008**, *231*, 157.
45. Wilson, I. B.; Ginsburg, S. *Biochim. Biophys. Acta* **1955**, *18*, 168.
46. Luettringhaus, A.; Hagedorn, I. *Arzneimittelforschung* **1964**, *14*, 1.
47. Steck, T. L.; Kant, J. A. Preparation of impermeable ghosts and inside-out vesicles from human erythrocyte membranes. In *Methods in Enzymology, Biomembranes, Part A*; Fleisher, S., Packer, L., Eds.; Academic Press Inc.: New York, 1974; Vol. XXXI, p 172.
48. Ellman, G. L.; Courtney, K. D.; Andres, V., Jr.; Featherstone, R. M. *Biochem. Pharmacol.* **1961**, *7*, 88.
49. Eyer, P.; Worek, F.; Kiderlen, D.; Sinko, G.; Stuglin, A.; Simeon-Rudolf, V.; Reiner, E. *Anal. Biochem.* **2003**, *312*, 224.
50. Worek, F.; Mast, U.; Kiderlen, D.; Diepold, C.; Eyer, P. *Clin. Chim. Acta* **1999**, *288*, 73.
51. Eyer, P.; Hagedorn, I.; Klimmek, R.; Lippstreu, P.; Loffler, M.; Oldiges, H.; Spöhrer, U.; Steidl, I.; Szinicz, L.; Worek, F. *Arch. Toxicol.* **1992**, *66*, 603.
52. Worek, F.; Krichner, T.; Bäcker, M.; Szinicz, L. *Arch. Toxicol.* **1996**, *70*, 497.
53. Sanner, M. F. *J. Mol. Graphics Model.* **1999**, *17*, 57.
54. Gomori, G. Preparation of Buffers for Use in Enzyme Studies. In *Methods in Enzymology*; Colowick, S. P., Kaplan, N. O., Eds.; Academic Press Inc.: New York, 1955; Vol. I, p 138.
55. Albert, A.; Sergeant, E. P. *A Laboratory Manual*; Chapman and Hall: London, 1971. p 44.
56. Sinko, G.; Calic, M.; Kovarik, Z. *FEBS. Lett.* **2006**, *580*, 3167.

Please cite this article in press as: Valiveti, A. K.; et al. *Bioorg. Med. Chem.* (2015), http://dx.doi.org/10.1016/j.bmc.2015.05.027